Chapter 2

Crystal and molecular structure of bis [1,3-di(*p*-*n*- octyloxyphenyl) propane -1,3-dionato] copper(II)

2.1 Introduction

The programme of crystal structure analysis of disc-like metallo organic complexes was commenced with the study of bis [1,3-di(*p*-*n*- octyloxyphenyl) propane -1,3-dionato] copper(II), hereafter referred to as Cu-OC_8H_{17}. Figure 2.1 shows the structural formula of Cu-OC_8H_{17}. As described in the yrevious chapter, the molecule includes a 11-atom core and a fringe, which in this case is made up of four phenyl rings, each one substituted with an octyloxy chain at the respective para-position. Thus, in Cu-OC_8H_{17}, the substitution is symmetrical. With the presence of four alkyl chains, the fringe of the molecule includes four oxygen atoms.

It must be mentioned that although large number of X-ray investigations on the mesophase of discogens have been reported in the past, the solid/crystalline phase of discogens has not received much attention. The study of Cu-OC_8H_{17} described in this chapter appears to be the first, detailed X-ray analysis of the crystal structure of a discogen, using single crystals and three dimensional intensity data.

2.2 Experimental details

On heating, Cu-OC_8H_{17} was found to exhibit the following transitions:

$$\mathrm{C} \xrightarrow{83.5} \mathrm{D}_L \xrightarrow{177^\circ C} \mathrm{I}$$

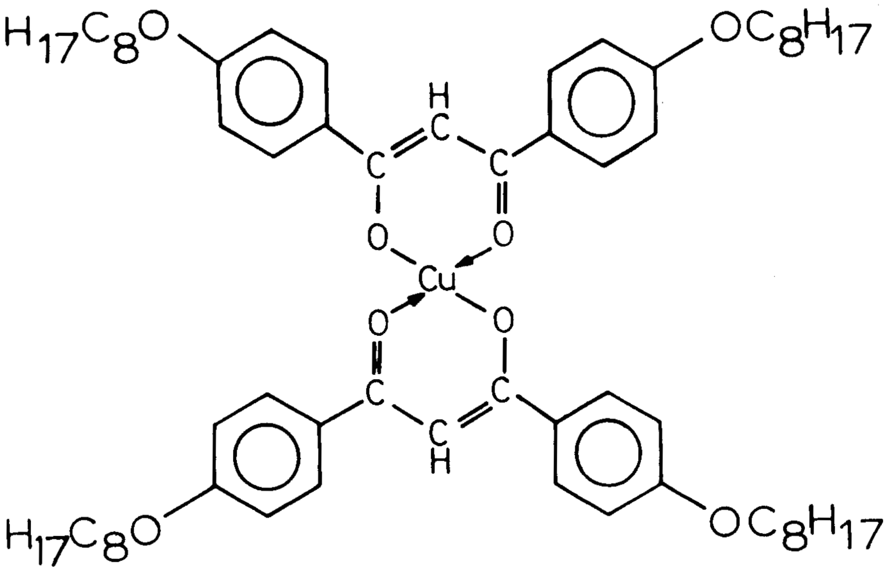

Figure 2.1: Structural formula.

where the symbols C, D_L and I represent the crystalline, discotic lamellar and the isotropic phases respectively. Green coloured, prismatic single crystals of Cu-OC_8H_{17} were obtained by slow evaporation from a solution in acetone. The unit cell dimensions were determined from oscillation and Weissenberg photographs and were later refined on a CAD4 single crystal diffractometer, using 21 reflections in the θ range of $8 < \theta < 35^\circ$. The crystal was found to belong to the triclinic system. Table 2.1 lists the crystal data. The estimated standard deviation, e.s.d, (o), of the a-axial length is 0.009Å and is considerably larger than the corresponding values of 0.001 and 0.002Å for the b and c-axial lengths. Possible correlation of the enhancement in the σ(a) with the molecular arrangement will be discussed later in this chapter. The value of ρ_{expt} showed that if the space group was P1, there are two independent molecules in the unit cell. If the space group was P$\bar{1}$, the asymmetric part of the unit cell includes only one molecule.

It must be pointed out that the measurement of the density, p, of Cu-OC_8H_{17} posed a serious problem. It was found that the crystals of Cu-OC_8H_{17} dissolved in most of the commonly available organic solvents. Also, the crystals exhibited remarkable hydrophobicity. Hence, finding suitable liquids for estimating the density by flotation method turned out to be the main hurdle. The value reported in Table 2.1 was obtained by flotation in a mixture of glycerol and absolute alcohol. On account of the viscous nature of glycerol, the measurement of p was very cumbersome. Despite the good agreement between the calculated (ρ_{calc}) and the measured (ρ_{expt}) values of density (Table 2.1), it was felt that the reliability of the measurement using glycerol was not very high.

Table 2.1: Crystal data.

Molecular formula	$C_{62}H_{86}O_8Cu$
Molecular weight	1022.8
a	11.300(9) Å
b	16.101(1) Å
c	17.089(2) Å
α	82.23(1) °
β	74.88(4) °
γ	77.43(3) °
V	2952Å^3
Space group	$P\bar{1}$
Z	2
ρ_{calc}	1.163 gm/cc
ρ_{expt}	1.164(3) gm/cc
μ_{CuK_α}	9.43 cm^{-1}
$F_{(000)}$	1102

Using a crystal of approximate dimensions 0.7x0.2×0.1mm^3, three dimensional intensity data were collected on a CAD4 diffractometer, in the $\omega/2\theta$ scan mode. nickel filtered CuK_α radiation (λ=1.5418Å) was used. The prescan speed used was 4.1°/minute. However, for the final scan, the speed was varied for each reflection to satisfy the relation $\frac{\sigma(I)}{I} \leq 0.03$ where $\sigma(I)$ is the estimated standard deviation for the measured intensity, I. During data collection, 114 and 201 were used as intensity control reflections and 252, $2\bar{3}4$ and 236 as the orientation control reflections. The former set looks for any deterioration in the quality of the crystal and the latter set checks the alignment of the crystal. Both deterioration of the crystal and misalignment during data collection could introduce significant reductions in the diffracted intensities. These problems are very common in the case of protein crystals which suffer easy radiation damage, and further, as they are mounted with the mother liquor, the chances of misalignment during data collection are also high. In the present experiments with the Cu-OC_8H_{17} crystal, the intensities of the control reflections were checked once after every 3600 seconds and it was found that till the end of the data collection, their intensities did not vary significantly.

In the θ range of 1 to 47°, intensities of 5217 independent reflections were measured of which 4043 reflections had I $\geq 3\sigma$(I). Table 2.2 describes the details of the data collection. The intensities were corrected for Lorentz and polarization factors.

Table 2.2: Details of data collection.

Radiation used	CuK_α
Crystal size	0.7x0.2x0.1mm^3
Scan mode	$\omega/2\theta$
Maximum Bragg angle	47°
Number of unique reflections	5217
Number of reflections with $I \geq 3\sigma(I)$	4043
Ranges of h	0 to 10
k	-14 to 15
l	-15 to 16

2.3 Structure determination and refinement

The crystal structure was solved by direct methods using MULTAN-80 [Germain *et al*, 19711, a program widely used and well known to the crystallographic community. The statistical distribution of E's presented in Table **2.3** shows the structure to be centrosymmetric. In fact, the distribution is close to the calculated values for a hypercentric structure. Hence, the space group was chosen to be Pi. With two molecules in the unit cell, the asymmetric part includes one formula unit *i.e.*, $C_{62}H_{86}O_8Cu$.

492 reflections with $|E| \geq 1.65$ and 100 reflections with the lowest E values were used to set up the phase relationships. In Table 2.4, details of the origin defining reflections and symbols are given. With six reflections in the starting set, there are 2^6 (=64) possible solutions. The summary of the figures of merit (FOM) output by MULTAN is given in Table 2.5.

The absolute figure of merit (ABS FOM) given in Table 2.5 is given by the following equation:

$$ABS\ FOM = \frac{Z - Z_{rand}}{Z_{exp} - Z_{rand}} \tag{2.1}$$

where,

$$Z = \sum_h \alpha_h$$

and α_h is defined by

$$\alpha_h = 2N^{-\frac{1}{2}}|E_h|(T_h^2 + B_h^2)^{\frac{1}{2}}$$

Table 2.3: Distribution of the normalized structure factors, E_{hkl}'s.

	Experimental	Theoretical		
average	all data	acentric	centric	hypercentric
$\|E\|$	0.734	0.886	0.798	0.718
E^2	1.000	1.000	1.000	1.000
E^3	2.032	1.329	1.596	1.916
E^4	5.912	2.000	3.000	4.500
E^5	24.031	3.323	6.383	12.260
E^6	127.980	6.000	15.000	37.500
$\|E^2\text{-}1\|$	1.103	0.736	0.968	1.145
$(E^2 - 1)^2$	4.912	1.000	2.000	3.500
$(E^2 - 1)^3$	112.245	2.000	8.000	26.000
$\|E^2\text{-}1\|^3$	113.076	2.415	8.691	26.903

Table 2.4: Details of the origin defining and the starting set of reflections.

h	k	1	E_{hkl}	
8	0	3	6.344	origin
3	2	5	5.362	origin
6	$\bar{3}$	$\bar{7}$	4.936	origin
2	2	4	8.315	starting set
1	4	1	4.759	starting set
4		2	4.581	starting set
4	$\bar{4}$	0	4.042	starting set
3	$\overline{10}$	$\bar{2}$	3.997	starting set
4	$\bar{9}$	3	3.786	starting set

Table 2.5: Summary of the figures of merit(FOM) output by the tangent formula.

	ABS FOM	PSI ZERO	R_{Karle}	COM FOM
Maximum value	1.1844	4.083	0.27	2.3207
Minimum value	0.6988	1.927	0.072	0.2452
Relative weights w_1, w_2, w_3 for COM FOM	0.60	1.20	1.20	

where

$$\frac{T_h}{B_h} = tan\phi_h \frac{\sum_{h'} (w_{h'}w_{h-h'}|E_{h'}E_{h-h'}|/(1-|U_h|^2))\, sin(\phi_{h'}+\phi_{h-h'})}{\sum_{h'} (w_{h'}w_{h-h'}|E_{h'}E_{h-h'}|/(1-|U_h|^2))\, cos(\phi_{h'}+\phi_{h-h'})}$$

and

$$w_h = tanh\left(\frac{1}{2}\alpha_h\right)$$

$$Z_{exp} = \sum_h \left\langle \alpha_h^2 \right\rangle_{exp}^{1/2}$$

$$\left\langle \alpha_h^2 \right\rangle_{exp} = \sum_{h'} K_{hh'}^2 + 2\sum_{h'}\sum_{h''} K_{hh'}K_{hh''} \frac{I_1(K_{hh'})}{I_0(K_{hh'})}\frac{I_1(K_{hh''})}{I_0(K_{hh''})}.$$

Here, I_0 and I_1 are modified Bessel functions.

$$(a{:})_{rand} = \sum_{h'} K_{hh'}^2$$

$$Z_{rand} = \sum_h \left\langle \alpha_h^2 \right\rangle_{rand}^{1/2}$$

$$K_{hh'} = 2\sigma_3\sigma_2^{-3/2}|E_hE_{h'}E_{h-h'}|$$

and

$$\sigma_n = \sum_{j=1}^{N} Z_j^n$$

The figure of merit PSI ZERO (ψ_0) is defined as,

$$\psi_0 = \sum_h |\sum_{h'} E_{h'}E_{h-h'}|$$

where the inner summation is over all terms available from the set of phases being determined and the outer summation is over a number of reflections for which

E_h is zero or small in magnitude. For a good set of phases the expected value of ψ_0 is small since the inner summation is essentially a selection of contributers to Sayre's equation.

The figure of merit R_{Karle} is given by,

$$R = \frac{\sum_h \left| |E_h|_{obs} - |E_h|_{cal} \right|}{\sum_h |E_h|_{obs}}$$

A combined figure of merit COM FOM based on Z, ψ_0 and R_{Karle} is given by,

$$COM\ FOM = w_1 \frac{Z - Z_{min}}{Z_{max} - Z_{min}} + w_2 \frac{(\psi_0)_{max} - \psi_0}{(\psi_0)_{max} - (\psi_0)_{min}} + w_3 \frac{R_{max} - R}{R_{max} - R_{min}}$$

where w_1, w_2 and w_3 are the weights given to Z, ψ_0 and R_{Karle} respectively.

Examination of the E-may corresponding to the set with the highest value of COM FOM did not yield the structure solution. Subsequent examination of E-maps corresponding to the solutions with the highest value of (i) ABS FOM and (ii) the lowest value of R_{Karle} were not useful either. The copper atom and 49 other nonhydrogen atoms, however, were identified from the solution corresponding to second lowest R_{Karle} value *viz.*, R=0.075. This set corresponds to the eighth best, value of COM FOM and the second best value of ABS FOM.

The positional and the isotropic thermal parameters of these 50 atoms were refined by block diagonal least squares procedure using a modified version of the program SFLS written originally by Shiono. The atomic scattering factors used in the calculations were those of Cromer and Waber [1965]. The R-factor defined as

$$R = \frac{\sum \left| |F_o| - |F_c| \right|}{\sum |F_o|}$$

reduced to 0.377 after five cycles of refinement. From a difference electron density map computed at this stage, 12 out of the remaining 21 atoms were located. With the inclusion of these atoms and subsequent introduction of anisotropic thermal parameters of the form,

$$exp\left[-\frac{1}{4}(B_{11}h^2a^{*2}+B_{22}k^2b^{*2}+B_{33}l^2c^{*2}+2B_{12}hka^*b^*+2B_{13}hla^*c^*+2B_{23}klb^*c^*)\right]$$

the R-value reduced to 0.197. A difference Fourier computed at this stage enabled identification of the remaining nine atoms, all of which belong to the terminal regions of two of the octyloxy chains. Introduction of these nine atoms in the least squares refinement brought down the R-value to 0.128. Until this stage of refinement, unit weighting scheme was used.

All the hydrogen atoms in the molecule were fixed geometrically, using a C-H distance of 1.08Å. The hydrogen atoms were assigned the equivalent isotropic temperature factor (B_{eq}) [Hamilton, 1959], defined as

$$B_{eq}=\frac{4}{3}\sum_{i=1}^{3}\sum_{j=1}^{3}B_{ij}\;(a_i\;.\;a_j)$$

of the respective carbon atoms to which they were covalently bonded. They were also assigned the same number as the carbon atom to which they are bonded (example: the hydrogen atom bonded to the carbon atom C(6) is referred to as H(6). When more than one hydrogen atom is bonded to a carbon atom, a second digit is added i.e., H(61) and H(62)). The same numbering scheme was adopted for all the seven crystal structures. The parameters of the hydrogen atoms were not refined. Their contribution to the structure factors were, however, included. After the inclusion of the hydrogen atoms and also the weighting function of the form

$$w = \frac{1}{(a_o + b_o F_o + c_o F_o^2)} \tag{2.2}$$

(where a_o=0.632, b_o=0.1'72 and c_o=-0.0002), the weighted R-value, R_w, defined

$$R_w = \left[\frac{\sum w\ (\ |F_o|\ -\ |F_c|\ )^2}{\sum w\ F_o^2} \right]^{\frac{1}{2}}$$

converged to 0.097 in 6 cycles. In the terminal cycle, the shifts, A's, of all the parameters were less than the corresponding e.s.d's, a. The highest value of Δ/σ was 0.108 for the parameter B_{33} of C(53).

During the course of the least squares refinement, it was observed that for the most intense reflection 224, the value of $|F_o|$ was much less than $|F_c|$ *viz.*, 469.5 and 545.8 respectively. This feature suggested the reflection being affected by secondary extinction effect. The intensity of the reflection 224 was corrected for secondary extinction using the formula [Zachariasen, 1963],

$$F_{corr} = K\ F_{obs}(1 + \beta_{(2\theta)}\ .\ g\ .\ I_{obs}) \tag{2.3}$$

where F_{obs} is the observed value of structure factor, I_{obs} is the observed integrated intensity and K is the scale factor.

$$g = \frac{\frac{I_{calc}}{I_{obs}} - 1}{2 I_{calc}} \tag{2.4}$$

where I_{calc} is the calculated intensity.

$$\beta_{(2\theta)} = \frac{2(1 + \cos^4(28))A^{*\prime}(20)}{(1 + \cos^2 2\theta)^2\ \ A^{*\prime}(0)} \tag{2.5}$$

where θ is the Bragg angle for the reflection 224, $A^{*1}(2\theta)$ is the absorption factor corresponding to the 20 and $A^{*\prime}$ is the absorption factor corresponding to $2\theta=0$.

In Table 2.6, some of the details of the least squares refinement are presented. In the course of the least squares refinement, the thermal parameters of the atoms C(22) to C(25) and C(51) to C(55), which correspond to the terminal regions of two of the octyloxy chains (Figure 2.2) were found to be rather high. Also, the molecular dimensions involving these atoms were found to deviate significantly from the expected values. Interestingly, these are the atoms whose positions were not readily identified from either the E-map or the subsequent difference Fourier. These features suggested the possibility of the presence of disorder in the chains which include the above mentioned atoms. Hence a difference electron density map removing the contribution from these nine atoms was computed. In the map, the electron density distribution was indeed diffuse. Attempts were made to identify possible alternative positions for these nine atoms. Molecular models were fitted on the diffuse electron density and occupancy factors of the newly fitted positions were refined by least squares method. There was however, no conclusive evidence for the presence of positionally resolvable disorder. It was therefore concluded that the high thermal parameters and the unusual molecular dimensions were due to the existance of alternative positions separated by distances too small to be resolved by X-ray analysis.

2.4 Results and discussion

Although the two halves of the molecule are chemically identical, they are not related by crystallographic symmetry elements. Table 2.7 lists the positional and equivalent temperature factor B_{eq} for all the nonhydrogen atoms. Table 2.8

Table 2.6: Some details of the refinement.

Weighting scheme	$1/(a_o+b_oF_o+c_oF_o^2)$
a_o	0.632
b_o	0.172
c_o	-0.0002
R_w for 4043 reflections with $I \geq 3\sigma(I)$	0.097
Maximum shift/e.s.d, Δ/σ	0.108

Table 2.7: Fractional coordinates and the B_{eq} (Å^2) values of the nonhydrogen atoms. The quantities in the parantheses are the respective e.s.d's.

Atom	x	y	z	B_{eq}	Atom	x	Y	z	B_{eq}
Cu	0.7692(2)	0.4120(1)	0.0424(2)	6.0	C(36)	0.668(2)	0.596(1)	-0.512(1)	6.5
O(1)	0.880(1)	0.4683(7)	-0.0408(7)	5.7	C(37)	0.790(2)	0.538(1)	-0.542(1)	6.9
O(2)	0.639(1)	0.5099(7)	0.0512(7)	5.7	C(38)	0.876(2)	0.574(1)	-0.617(1)	7.2
O(3)	0.658(1)	0.3554(7)	0.1241(7)	5.2	C(39)	0.999(2)	0.515(1)	-0.645(1)	7.4
O(4)	0.897(1)	0.3147(6)	0.0343(7)	5.5	C(40)	2.086(2)	0.554(2)	-0.715(2)	9.2
C(5)	0.856(2)	0.544(1)	-0.072(1)	4.8	C(41)	0.516(2)	0.641(1)	0.025(1)	4.4
C(6)	0.741(2)	0.599(1)	-0.052(1)	4.9	C(42)	0.500(1)	0.728(1)	-0.005(1)	4.5
C(7)	0.638(1)	0.579(1)	0.008(1)	4.4	C(4.3)	0.386(2)	0.781(1)	0.017(1)	4.9
C(8)	(I)	0.244(1)	0.071(1)	4.4	C(44)	0.285(2)	0.750(1)	0.068(1)	4.6
C(9)	0.792(2)	0.220(1)	0.130(1)	5.1	C(45)	0.298(2)	0.665(1)	0.098(1)	5.4
C(10)	0.679(2)	0.278(1)	0.152(1)	5.0	C(46)	0.415(2)	0.613(1)	0.076(1)	4.7
C(11)	0.013(2)	0.177(1)	0.050(1)	4.5	O(47)	0.178(1)	0.8094(7)	0.0882(7)	6.0
C(12)	0.024(2)	0.089(1)	0.063(1)	4.9	C(48)	0.076(2)	0.781(1)	0.147(1)	6.2
C(13)	0 (2	0.035(1)	0.032(1)	5.1	C(49)	-0.022(2)	0.862(1)	0.167(1)	7.1
C(14)	0.240(2)	0.069(1)	-0.011(1)	5.1	C(50)	-0.141(2)	0.831(2)	0.232(2)	11.8
C(15)	0.231(2)	0.156(1)	-0.022(1)	5.2	C(51)	-0.234(3)	0.911(3)	0.259(2)	14.3
C(16)	0.120(2)	0.209(1)	0.008(1)	5.4	C(52)	-0.344(4)	0.872(4)	0.331(3)	25.4
O(17)	0.343(1)	0.0078(7)	-0.0404(7)	6.2	C(53)	-0.397(7)	0.909(4)	0.374(3)	26.1
C(18)	0.445(2)	0.042(1)	-0.093(1)	6.2	C(54)	-0.514(6)	0.844(4)	0.448(3)	22.8
C(19)	0.539(2)	-0.039(1)	-0.130(1)	6.6	C(55)	-0.569(6)	0.912(4)	0.441(3)	24.5
C(20)	0.655(2)	-0.004(2)	-0.185(1)	9.1	C(56)	0.570(2)	0.254(1)	0.216(1)	4.7
C(21)	0.754(2)	-0.076(2)	-0.220(2)	11.7	C(57)	0.454(2)	0.308(1)	0.224(1)	5.5
C(22)	0.877(4)	-0.029(3)	-0.280(2)	15.5	C(58)	0.351(2)	0.294(1)	0.283(1)	5.5
C(23)	0.957(7)	-0.085(3)	-0.315(3)	27.2	C(59)	0.360(2)	0.222(1)	0.337(1)	5.S
C(24)	2.050(6)	-0.028(5)	-0.376(4)	29.3	C(60)	0.474(2)	0.164(1)	0.330(1)	6.2
C(25)	2.125(6)	-0.071(6)	-0.390(6)	35.5	C(61)	0.575(2)	0.179(1)	0.270(1)	5.9
C(26)	0.964(2)	0.571(1)	-0.136(1)	4.6	O(62)	0.267(1)	0.2018(8)	0.4008(8)	7.2
C(27)	0.955(2)	0.650(1)	-0.183(1)	5.4	C(6.3)	0.151(2)	0.260(1)	0.415(1)	7.1
C(28)	0.056(2)	0.669(1)	-0.241(1)	5.6	C(64)	0.071(2)	0.225(1)	0.495(1)	7.0
C(29)	0.171(2)	0.613(1)	-0.252(1)	5.1	C(65)	-0.062(2)	0.281(1)	0.510(1)	7.9
C(30)	0.180(2)	0.536(1)	-0.206(1)	5.3	C(66)	-0.143(2)	0.251(1)	0.593(1)	7.4
C(31)	0.078(2)	0.517(1)	-0.148(1)	5.0	C(67)	-0.270(2)	0.307(1)	0.616(1)	7.4
O(32)	0.265(1)	0.6386(8)	-0.3122(8)	6.6	C(68)	-0.351(2)	0.274(1)	0.696(1)	7.2
C(33)	0.382(2)	0.581(1)	-0.330(1)	5.8	C(69)	-0.481(2)	0.331(2)	0.719(1)	9.1
C(34)	0.462(2)	0.620(1)	-0.406(1)	6.6	C(70)	-0.565(2)	0.294(2)	0.793(1)	9.1
C(35)	0.588(2)	0.561(1)	-0.435(1)	6.8					

Table 2.8: Anisotropic thermal parameters B_{ij} of the nonhydrogen atoms.

Atom	B_{11}	B_{22}	B_{33}	B_{12}	B_{13}	B_{23}
Cu	0.0130(3)	0.0041(1)	0.0062(1)	0.0008(2)	-0.0011(2)	0.0004(1)
O(1)	0.012(1)	0.0030(5)	0.0065(6)	0.0008(7)	-0.0009(7)	0.0013(5)
O(2)	0.013(1)	0.0029(5)	0.0062(6)	0.0001(7)	-0.0001(7)	0.0009(4)
O(3)	0.011(1)	0.0036(5)	0.0054(6)	0.0003(7)	-0.0008(7)	0.0008(4)
O(4)	0.014(1)	0.0026(5)	0.0060(6)	0.0002(7)	-0.0014(7)	0.0009(4)
C(5)	0.009(2)	0.0050(9)	0.0046(8)	0.000(1)	-0.001(1)	-0.0009(7)
C(6)	0.009(2)	0.0038(9)	0.0055(9)	0.001(1)	-0.001(1)	0.0008(7)
C(7)	0.008(2)	0.0031(8)	0.0055(9)	-0.0004(9)	-0.001(1)	-0.0004(7)
C(8)	0.008(2)	0.0046(9)	0.0044(8)	-0.001(1)	-0.001(1)	-0.0006(7)
C(9)	0.012(2)	0.0035(8)	0.0050(9)	0.002(1)	-0.003(1)	0.0002(7)
C(10)	0.013(2)	0.0040(9)	0.0044(8)	0.001(1)	-0.002(1)	-0.0005(7)
C(11)	0.009(2)	0.0044(9)	0.0041(8)	0.000(1)	-0.001(1)	0.0000(7)
C(12)	0.011(2)	0.0031(8)	0.0054(9)	0.000(1)	-0.002(1)	0.0004(7)
C(13)	0.012(2)	0.0030(8)	0.0057(9)	0.001(1)	-0.002(1)	-0.0001(7)
C(14)	0.009(2)	0.0046(9)	0.0054(9)	-0.000(1)	-0.001(1)	0.0000(7)
C(15)	0.011(2)	0.0031(8)	0.007(1)	-0.001(1)	-0.002(1)	0.0006(7)
C(16)	0.011(2)	0.0033(8)	0.007(1)	0.001(1)	-0.002(1)	-0.0003(7)
O(17)	0.011(1)	0.0046(6)	0.0067(7)	0.002(7)	0.0005(8)	-0.0001(5)
C(18)	0.011(2)	0.006(1)	0.006(1)	0.002(1)	-0.001(1)	-0.0002(8)
C(19)	0.010(2)	0.008(1)	0.005(1)	0.002(1)	-0.001(1)	-0.0015(9)
C(20)	0.015(3)	0.011(2)	0.006(1)	0.002(2)	-0.000(2)	-0.0010(1)
C(21)	0.015(3)	0.017(3)	0.009(2)	0.001(2)	0.000(2)	-0.004(2)
C(22)	0.030(6)	0.017(3)	0.014(2)	-0.001(3)	0.001(3)	-0.006(2)
C(23)	0.10(2)	0.014(4)	0.017(4)	-0.007(7)	0.000(7)	-0.006(6)
C(24)	0.05(1)	0.04(1)	0.020(5)	-0.020(9)	0.005(6)	-0.009(6)
C(25)	0.05(1)	0.04(1)	0.038(9)	-0.03(1)	0.013(9)	-0.014(8)
C(26)	0.011(2)	0.0036(8)	0.0040(8)	0.001(1)	-0.002(1)	-0.0002(6)
C(27)	0.011(2)	0.0047(9)	0.0053(9)	0.001(1)	-0.002(1)	-0.0007(7)
C(28)	0.010(2)	0.005(1)	0.0053(9)	0.000(1)	-0.000(1)	0.0007(8)
C(29)	0.009(2)	0.006(1)	0.0047(9)	-0.001(1)	-0.001(1)	-0.0002(7)
C(30)	0.010(2)	0.0041(9)	0.0057(9)	-0.000(1)	-0.001(1)	0.0002(7)
C(31)	0.010(2)	0.0040(9)	0.0049(9)	-0.000(1)	-0.000(1)	0.0010(7)
O(32)	0.011(1)	0.0064(7)	0.0062(7)	-0.0007(8)	0.0007(8)	0.0006(5)
C(33)	0.010(2)	0.006(1)	0.0054(9)	-0.000(1)	-0.000(1)	-0.0004(8)
C(34)	0.013(2)	0.007(1)	0.0049(9)	-0.001(1)	0.001(1)	0.0005(8)
C(35)	0.013(3)	0.007(1)	0.006(1)	-0.001(1)	-0.000(1)	-0.0002(9)

...(contd.)

Table 2.8 continued...

Atom	B_{11}	B_{22}	B_{33}	B_{12}	B_{13}	B_{23}
C(36)	0.013(2)	0.007(1)	0.005(1)	-0.001(1)	-0.000(1)	0.0003(8)
C(37)	0.015(3)	0.007(1)	0.005(1)	-0.000(1)	-0.001(1)	-0.0004(9)
C(38)	0.015(3)	0.008(1)	0.006(1)	-0.002(2)	-0.000(1)	-0.0004(9)
C(39)	0.013(3)	0.009(1)	0.006(1)	-0.001(2)	0.001(1)	-0.001(1)
C(40)	0.017(3)	0.011(2)	0.008(1)	-0.003(2)	0.001(2)	-0.003(1)
C(41)	0.010(2)	0.0031(8)	0.0046(8)	-0.000(1)	-0.001(1)	-0.0003(6)
C(42)	0.008(2)	0.0041(9)	0.0045(8)	0.001(1)	-0.001(1)	-0.0000(7)
C(43)	0.008(2)	0.0038(8)	0.0056(9)	0.001(1)	-0.001(1)	0.0005(7)
C(44)	0.009(2)	0.0042(9)	0.0047(8)	0.000(1)	-0.002(1)	-0.0005(7)
C(45)	0.010(2)	0.0043(9)	0.0057(9)	0.000(1)	-0.001(1)	0.0008(7)
C(46)	0.009(2)	0.0032(8)	0.0053(9)	0.000(1)	-0.001(1)	0.0006(7)
O(47)	0.010(1)	0.0047(6)	0.0062(6)	0.0014(7)	0.0009(7)	0.0000(5)
C(48)	0.012(2)	0.006(1)	0.0049(9)	0.000(1)	-0.000(1)	0.0000(8)
C(49)	0.011(2)	0.008(1)	0.006(1)	0.002(1)	0.002(1)	-0.0002(9)
C(50)	0.017(4)	0.014(2)	0.010(2)	-0.002(2)	0.004(2)	-0.002(2)
C(51)	0.015(4)	0.022(4)	0.012(2)	0.002(3)	-0.000(2)	-0.008(2)
C(52)	0.025(6)	0.040(7)	0.024(4)	-0.011(5)	0.011(4)	-0.023(5)
C(53)	0.08(2)	0.024(5)	0.013(3)	-0.008(8)	0.005(6)	-0.006(3)
C(54)	0.06(1)	0.024(5)	0.011(3)	0.006(6)	-0.004(5)	-0.005(3)
C(55)	0.07(1)	0.020(5)	0.016(4)	-0.008(7)	0.004(6)	-0.003(3)
C(56)	0.011(2)	0.0040(9)	0.0042(8)	0.000(1)	-0.002(1)	-0.0003(7)
C(57)	0.012(2)	0.0047(9)	0.0047(9)	-0.001(1)	0.000(1)	0.0015(7)
C(58)	0.011(2)	0.005(1)	0.0054(9)	-0.000(1)	-0.001(1)	0.0012(7)
C(59)	0.012(2)	0.005(1)	0.0051(9)	-0.001(1)	-0.000(1)	-0.0003(8)
C(60)	0.015(3)	0.005(1)	0.0045(9)	-0.000(1)	0.001(1)	0.0014(7)
C(61)	0.014(2)	0.0043(9)	0.0051(9)	0.002(1)	-0.002(1)	0.0003(7)
O(62)	0.014(2)	0.0067(8)	0.0060(7)	-0.0011(9)	0.0015(8)	0.0010(6)
C(63)	0.014(3)	0.007(1)	0.006(1)	-0.000(1)	-0.000(1)	-0.0004(9)
C(64)	0.012(2)	0.006(1)	0.007(1)	0.000(1)	0.002(1)	-0.0003(9)
C(65)	0.016(3)	0.007(1)	0.007(1)	-0.003(2)	-0.000(2)	0.000(1)
C(66)	0.017(3)	0.007(1)	0.006(1)	-0.001(2)	-0.000(1)	0.0004(9)
C(67)	0.013(3)	0.009(1)	0.006(1)	-0.000(2)	-0.000(1)	-0.000(1)
C(68)	0.014(3)	0.008(1)	0.006(1)	-0.002(2)	-0.000(1)	-0.0001(9)
C(69)	0.017(3)	0.011(2)	0.006(1)	-0.001(2)	0.000(2)	0.000(1)
C(70)	0.019(3)	0.010(2)	0.007(1)	-0.001(2)	0.000(2)	-0.002(1)

lists the anisotropic thermal parameters B_{ij}'s. The positional and the isotropic temperature factors of the hydrogen atoms are given in Table 2.9.

Figure 2.2 shows the thermal ellipsoids plotted with 50% probability using the program ORTEP [Johnson, 1976] and also the atomic numbering scheme. The average value of B_{eq} for the 11-atom core of the molecule (comprising of the atoms Cu, O(1) to O(4), C(5) to C(10)) is 5.2(5)Å^2. In the phenyl rings A and D (Figure 2.2) the B_{eq} values average to 5.2(3), 5.2(3), 5.6(5) and 4.8(3)Å^2 repectively and are comparable to that of the core. On moving further away from the core *i.e.*, towards the octyloxy chains, the thermal parameters register a conspicuous increase. The octyloxy chains A to D are characterized by average B_{eq} values of 7.0(9), 16(11), 7.7(8) and 16(8)Å^2 respectively. It is very striking that the thermal parameters of the chains B and D are significantly larger than those of A and C. It must be pointed out that the nine atoms for which the thermal parameters were found to be high during refinement, belong to the chains B and D. Examination of the molecular arrangement (to be described subsequently) shows that the octyloxy chains A and C point towards the aromatic, central regions of the molecules in the neighbouring unit cells. The chains B and D on the other hand point towards the octyloxy chains. The difference in the type of packing of the octyloxy chains seems to have a significant bearing on their respective B_{eq} values. Further, it is also well known that in the discotic mesophase, the chains which form the fringe of disc-like molecules are likely to be flexible and disordered. It is therefore likely that the high thermal parameters of chains B and D observed in the crystalline state are perhaps indicative of similar disorder which may be present in the mesophase of Cu-OC_8H_{17}. Similar high thermal

Table 2.9: Fractional coordinates and the B_{iso} (Å^2) values of hydrogen atoms.

Atom	x	y	z	B_{iso}	Atom	x	y	z	B_{iso}
H(6)	0.732	0.660	-0.088	4.8	H(403)	2.037	0.571	-0.766	10.1
H(9)	0.799	0.154	0.157	4.6	H(42)	0.578	0.752	-0.045	4.2
H(12)	0.941	0.059	0.095	5.3	H(43)	0.372	0.846	-0.008	4.6
H(13)	0.143	-0.034	0.043	4.8	H(45)	0.216	0.639	0.134	5.2
H(15)	0.315	0.183	-0.053	5.3	H(46)	0.428	0.545	0.097	4.6
H(16)	0.116	0.278	-0.001	5.2	H(481)	0.102	0.749	0.201	6.8
H(181)	0.425	0.068	-0.150	6.0	H(482)	0.036	0.736	0.118	6.8
H(182)	0.535	0.004	-0.081	6.0	H(491)	-0.088	0.851	0.225	6.7
H(191)	0.558	0.934	0.928	6.7	H(492)	-0.038	0.898	0.110	6.7
H(192)	0.454	0.001	0.857	6.7	H(501)	0.926	0.848	0.173	11.2
H(201)	0.693	0.030	0.853	8.5	H(502)	0.881	0.790	0.284	11.2
H(202)	0.628	0.041	0.768	8.5	H(511)	0.720	0.936	0.209	14.8
H(211)	0.718	0.890	0.743	10.7	H(512)	0.803	0.954	0.283	14.8
H(212)	0.791	0.882	0.828	10.7	H(521)	0.717	0.821	0.371	21.1
H(221)	0.901	0.010	0.754	14.3	H(522)	0.627	0.821	0.308	21.1
H(222)	0.838	0.007	0.667	14.3	H(531)	0.523	0.959	0.339	22.7
H(231)	0.933	0.867	0.659	19.9	H(532)	0.613	0.947	0.415	22.7
H(232)	0.008	0.878	0.741	19.9	H(541)	0.520	0.828	0.489	21.2
H(241)	0.105	0.999	0.657	20.4	H(542)	0.465	0.810	0.400	21.2
H(242)	0.016	0.997	0.576	20.4	H(551)	0.309	0.886	0.497	25.9
H(251)	0.222	0.899	0.552	27.3	H(552)	0.355	0.944	0.403	25.9
H(252)	0.091	0.849	0.577	27.3	H(553)	0.406	0.961	0.487	25.9
H(253)	0.173	0.851	0.651	27.3	H(57)	0.444	0.366	0.182	5.4
H(27)	0.864	0.693	-0.174	5.4	H(58)	0.259	0.335	0.282	5.7
H(28)	0.046	0.731	-0.278	5.8	H(60)	0.483	0.107	0.373	6.2
H(30)	0.270	0.490	-0.215	4.8	H(61)	0.662	0.133	0.264	5.8
H(31)	0.085	0.457	-0.108	4.8	H(631)	0.109	0.260	0.362	8.0
H(331)	0.367	0.518	-0.342	5.4	H(632)	0.165	0.323	0.419	8.0
H(332)	0.427	0.573	-0.279	5.4	H(641)	0.066	0.158	0.489	6.8
H(341)	0.478	0.680	-0.394	7.2	H(642)	-0.000	0.275	0.523	6.8
H(342)	0.413	0.631	-0.455	7.2	H(651)	0.942	0.349	0.514	7.6
H(351)	0.571	0.499	-0.442	7.0	H(652)	0.942	0.349	0.514	7.6
H(352)	0.637	0.552	-0.386	7.0	H(661)	0.902	0.243	0.642	8.3
H(361)	0.687	0.657	-0.505	6.6	H(662)	0.844	0.185	0.587	8.3
H(362)	0.616	0.608	-0.561	6.6	H(671)	0.679	0.311	0.568	7.4
H(371)	0.769	0.477	-0.555	7.6	H(672)	0.739	0.371	0.622	7.4
H(372)	0.835	0.520	-0.492	7.6	H(681)	0.697	0.269	0.744	7.6
H(381)	0.894	0.634	-0.604	7.5	H(682)	0.636	0.209	0.690	7.6
H(382)	0.829	0.590	-0.668	7.5	H(691)	0.476	0.341	0.667	8.9
H(391)	0.982	0.455	-0.662	7.9	H(692)	0.532	0.394	0.730	8.9
H(392)	2.016	0.497	-0.594	7.9	H(701)	0.344	0.336	0.808	8.8
H(401)	2.171	0.512	-0.735	10.1	H(702)	0.477	0.285	0.845	8.8
H(402)	2.100	0.613	-0.699	10.1	H(703)	0.422	0.232	0.782	8.8

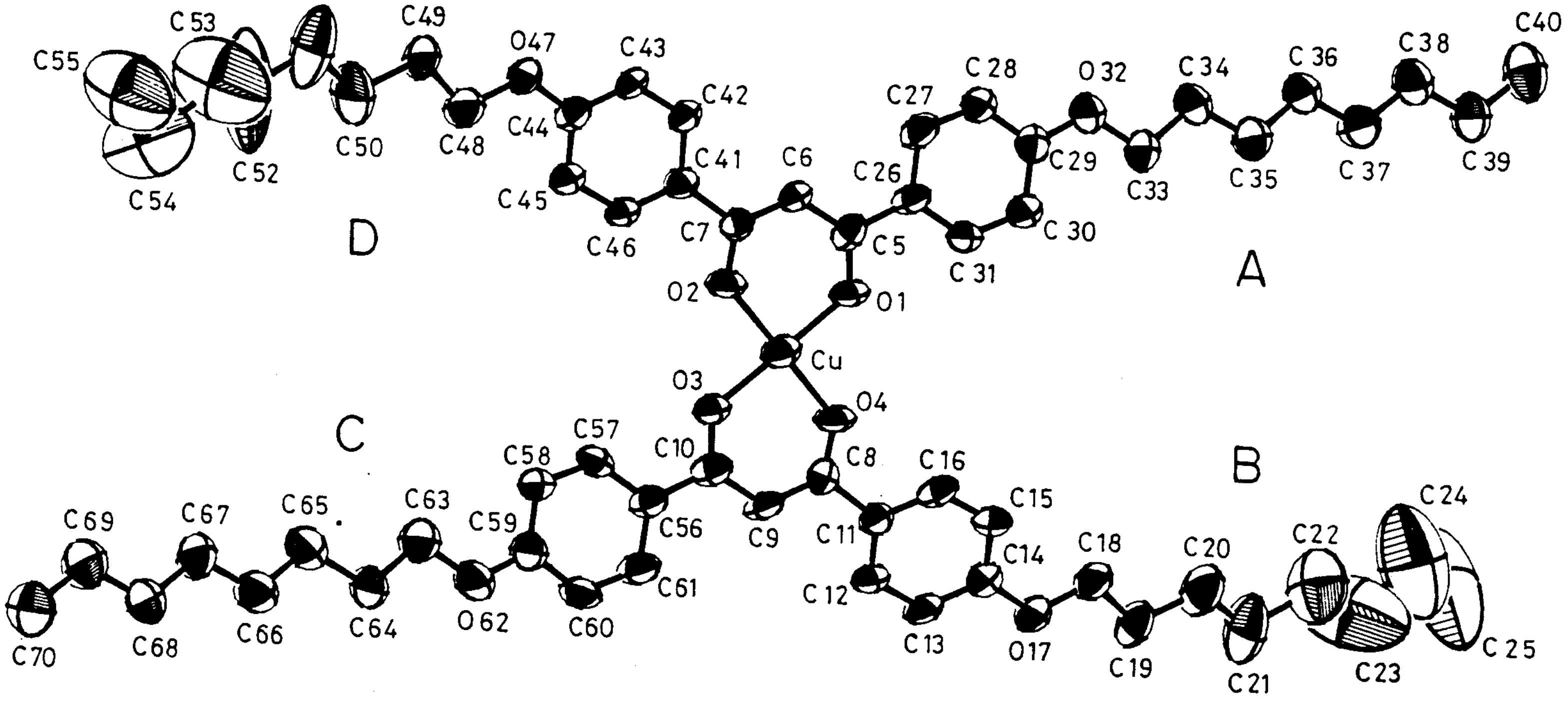

Figure 2.2: ORTEP diagram of the thermal ellipsoids drawn with 50% probability [Johnson, 1976].

vibrations and consequent abnormal molecular dimensions have been observed in the crystal structures of several other mesogens also [Polishchuk et al, 1986; Pattabhi and Craven, 1979; Leadbetter and Mazid, 1981].

In Table 2.10(a), (b) and (c) the individual bond lengths, bond angles and the average values for different groups of the molecule are listed. Comparison with the values given by Allen *et al* [1987], has also been made (Table 2.10(c)). Within limits of experimental error, the molecular dimensions are normal in all parts other than in chains B and D. The copper atom which occupies a general position in the unit cell is surrounded by four oxygen atoms which form a square planar arrangement. Figure 2.3 shows the coordination around the copper atom. It must be mentioned that the distances O(1)...O(4), O(2)...O(3) are shorter than the distances O(1)...O(2) and O(3)...O(4).

The structural formula in Figure 2.1 suggests that the 11-atom core of the molecule could be planar. Calculation of the least squares mean plane, however, shows that the 11-atom core is only nearly planar. It is found that the least squares plane through the atoms in one half of the core *viz.*, Cu, O(1), O(2), C(5) to C(7) makes an angle of 2° with that through the group of atoms in the other half *viz.*, Cu, O(3), O(4), C(8) to C(10). Calculation of the planes which do not include the metal atom *i.e.*, through O(1), O(2), C(5) to C(7) and O(3), O(4), C(8) to C(10) showed that the tilt between the two halves persisted as 5°. This feature shows that the buckling between the two halves cannot be attributed to the presence of the heavy metal atom at the geometric centre of the core.

Table 2.10(a): Bond lengths(Å)

Cu-O(1)	1.90(1)	O(32)-C(33)	1.43(2)
Cu-O(2)	1.90(1)	C(33)-C(34)	1.52(2)
Cu-O(3)	1.91(1)	C(34)-C(35)	1.53(3)
Cu-O(4)	1.879(9)	C(35)-C(36)	1.51(2)
O(1)-C(5)	1.26(2)	C(36)-C(37)	1.50(3)
O(2)-C(7)	1.25(2)	C(37)-C(38)	1.52(2)
O(3)-C(10)	1.27(2)	C(38)-C(39)	1.50(3)
O(4)-C(8)	1.22(2)	C(39)-C(40)	1.50(3)
C(5)-C(6)	1.39(3)	C(41)-C(46)	1.37(3)
C(5)-C(26)	1.51(3)	C(41)-C(42)	1.41(2)
C(6)-C(7)	1.40(2)	C(42)-C(43)	1.37(2)
C(7)-C(41)	1.50(2)	C(43)-C(44)	1.39(3)
C(8)-C(9)	1.42(2)	C(44)-O(47)	1.37(2)
C(8)-C(11)	1.51(2)	C(44)-C(45)	1.39(2)
C(9)-C(10)	1.40(3)	C(45)-C(46)	1.39(3)
C(10)-C(56)	1.50(3)	O(47)-C(48)	1.43(2)
C(11)-C(12)	1.39(2)	C(48)-C(49)	1.53(2)
C(11)-C(16)	1.40(3)	C(49)-C(50)	1.63(3)
C(12)-C(13)	1.39(2)	C(50)-C(51)	1.51(5)
C(13)-C(14)	1.39(3)	C(51)-C(52)	1.67(6)
C(14)-C(15)	1.37(2)	C(52)-C(53)	0.99(8)
C(14)-O(17)	1.38(2)	C(53)-C(54)	1.95(9)
C(15)-C(16)	1.37(2)	C(54)-C(55)	1.14(8)
O(17)-C(18)	1.43(2)	C(56)-C(57)	1.39(3)
C(18)-C(19)	1.58(2)	C(56)-C(61)	1.42(2)
C(19)-C(20)	1.57(3)	C(57)-C(58)	1.36(3)
C(20)-C(21)	1.49(4)	C(58)-C(59)	1.38(2)
C(21)-C(22)	1.75(5)	C(59)-O(62)	1.36(2)
C(22)-C(23)	1.22(6)	C(59)-C(60)	1.40(3)
C(23)-C(24)	1.62(9)	C(60)-C(61)	1.36(3)
C(24)-C(25)	1.0(1)	O(62)-C(63)	1.42(2)
C(26)-C(31)	1.37(3)	C(63)-C(64)	1.54(2)
C(26)-C(27)	1.41(2)	C(64)-C(65)	1.55(3)
C(27)-C(28)	1.36(3)	C(65)-C(66)	1.55(2)
C(28)-C(29)	1.39(3)	C(66)-C(67)	1.51(3)
C(29)-O(32)	1.36(2)	C(67)-C(68)	1.53(2)
C(29)-C(30)	1.37(2)	C(68)-C(69)	1.54(3)
C(30)-C(31)	1.37(3)	C(69)-C(70)	1.51(3)

Table 2.10(b): Bond angles(°)

O(4)-Cu-O(3)	92.3(5)	C(16)-C(15)-C(14)	120(2)	C(42)-C(43)-C(44)	121(2)
O(4)-Cu-O(2)	179.5(5)	C(15)-C(16)-C(11)	122(2)	O(47)-C(44)-C(45)	124(2)
O(4)-Cu-O(1)	87.8(5)	C(14)-O(17)-C(18)	114(1)	O(47)-C(44)-C(43)	115(2)
O(3)-Cu-O(2)	87.3(5)	O(17)-C(18)-C(19)	104(1)	C(45)-C(44)-C(43)	120(2)
O(3)-Cu-O(1)	179.2(5)	C(20)-C(19)-C(18)	105(2)	C(44)-C(45)-C(46)	118(2)
O(2)-Cu-O(1)	92.8(5)	C(21)-C(20)-C(19)	110(2)	C(41)-C(46)-C(45)	123(2)
C(5)-O(1)-Cu	126(1)	C(20)-C(21)-C(22)	106(2)	C(44)-O(47)-C(48)	116(1)
C(7)-O(2)-Cu	128(1)	C(23)-C(22)-C(21)	108(4)	O(47)-C(48)-C(49)	105(1)
C(10)-O(3)-Cu	127(1)	C(22)-C(23)-C(24)	101(5)	C(48)-C(49)-C(50)	106(2)
C(8)-O(4)-Cu	129(1)	C(25)-C(24)-C(23)	101(8)	C(51)-C(50)-C(49)	107(2)
O(1)-C(5)-C(6)	125(2)	C(31)-C(26)-C(27)	118(2)	C(50)-C(51)-C(52)	103(3)
O(1)-C(5)-C(26)	114(2)	C(31)-C(26)-C(5)	119(2)	C(53)-C(52)-C(51)	119(6)
C(6)-C(5)-C(26)	121(2)	C(27)-C(26)-C(5)	123(2)	C(52)-C(53)-C(54)	108(6)
C(5)-C(6)-C(7)	124(2)	C(28)-C(27)-C(26)	120(2)	C(55)-C(54)-C(53)	74(5)
O(2)-C(7)-C(6)	124(1)	C(27)-C(28)-C(29)	121(2)	C(57)-C(56)-C(61)	116(2)
O(2)-C(7)-C(41)	115(1)	O(32)-C(29)-C(30)	125(2)	C(57)-C(56)-C(10)	119(2)
C(6)-C(7)-C(41)	121(1)	C(30)-C(29)-C(28)	119(2)	C(61)-C(56)-C(10)	125(2)
O(4)-C(8)-C(9)	125(1)	O(32)-C(29)-C(28)	116(2)	C(58)-C(57)-C(56)	123(2)
O(4)-C(8)-C(11)	117(1)	C(31)-C(30)-C(29)	120(2)	C(57)-C(58)-C(59)	119(2)
C(9)-C(8)-C(11)	118(1)	C(30)-C(31)-C(26)	122(2)	O(62)-C(59)-C(58)	126(2)
C(10)-C(9)-C(8)	122(2)	C(29)-O(32)-C(33)	118(1)	O(62)-C(59)-C(60)	114(2)
O(3)-C(10)-C(9)	125(2)	O(32)-C(33)-C(34)	107(1)	C(58)-C(59)-C(60)	120(2)
O(3)-C(10)-C(56)	113(2)	C(33)-C(34)-C(35)	112(2)	C(61)-C(60)-C(59)	120(2)
C(9)-C(10)-C(56)	122(2)	C(36)-C(35)-C(34)	113(2)	C(60)-C(61)-C(56)	122(2)
C(12)-C(11)-C(16)	118(2)	C(37)-C(36)-C(35)	114(2)	C(59)-O(62)-C(63)	118(1)
C(12)-C(11)-C(8)	128(2)	C(36)-C(37)-C(38)	115(2)	O(62)-C(63)-C(64)	106(1)
C(16)-C(11)-C(8)	115(2)	C(39)-C(38)-C(37)	114(2)	C(63)-C(64)-C(65)	109(2)
C(11)-C(12)-C(13)	121(2)	C(40)-C(39)-C(38)	113(2)	C(64)-C(65)-C(66)	110(2)
C(12)-C(13)-C(14)	120(2)	C(46)-C(41)-C(42)	118(2)	C(67)-C(66)-C(65)	113(2)
C(15)-C(14)-O(17)	127(2)	C(46)-C(41)-C(7)	118(2)	C(66)-C(67)-C(68)	113(2)
C(15)-C(14)-C(13)	119(2)	C(42)-C(41)-C(7)	124(2)	C(67)-C(68)-C(69)	113(2)
O(17)-C(14)-C(13)	114(2)	C(43)-C(42)-C(41)	120(2)	C(70)-C(69)-C(68)	113(2)

Table 2.10(c): Average values of bond lengths(Å) and valence angles(°) fur different groups. Comparison with the values given by Allen *et al*, [1987] is also made.

	average bond lengths	values of Allen *et al*		average bond angles
Core:				
Cu-O	1.895(5)		O-Cu-O	92.6(2)
O-C_{ar}(core)	1.25(1)		Cu-O-C_{ar}	127.8(8)
C_{ar}-C_{ar} (core)	1.405(5)		O-C_{ar}-C_{ar}	124.3(4).
			C_{ar}-C_{ar}-C_{ar}	123(1)
Phenyl ring:				
A	1.38(2)	1.380(13)		120(1)
B	1.39(1)			120(1)
C	1.39(1)			120(2)
D	1.39(2)			120(2)
Chain:				
A	1.51(1)	1.530(15)		114(1)
B	1.5(2)			105(4)
C	1.54(1)			112(2)
D	1.5(3)			103(14)
O-C_{sp^3}	1.428(4)	1.450(14)	C_{phenyl}-O-C_{sp^3}	117(2)
O-C_{phenyl}	1.368(8)	1.370(11)	O-C_{sp^3}-C_{sp^3}	106(1)
C_{core}-C_{phenyl}	1.505(5)			

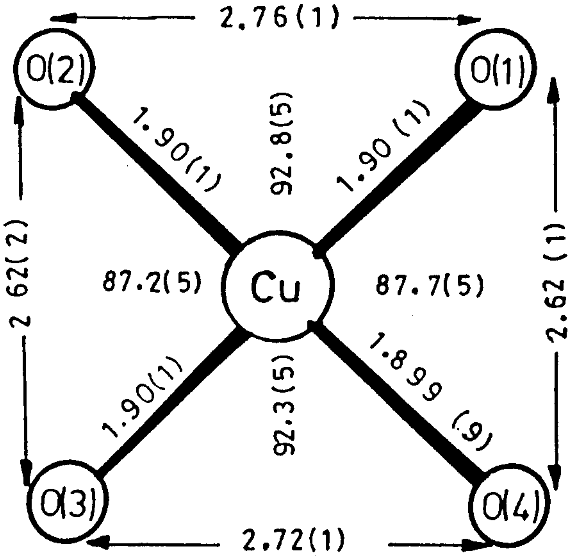

Figure 2.3: Coordination around the metal atom.

It is also observed that each half of the core, by itself is not strictly planar. The least squares plane through the atoms Cu, O(1), C(5) and C(6) is found to be inclined to the plane through the atoms Cu, O(2), C(7), and C(6) by 3". Similarly in the other half of the core, the plane through Cu, O(3), C(10) and C(9) is inclined by 1.5° to the plane through the atoms Cu, O(4), C(8) and C(9). The phenyl rings are found to be planar. The angles between the normals to the least squares planes of the phenyl rings and the 11-atom core are 7.4, 20.5, 12.0 and 8.0°. To calculate the average tilts of the octyloxy chains with respect to the core, least squares planes were fitted through the oxygen and the eight carbon atoms of each of the chains A to D. The tilts are 10.7, 23.5, 17.1 and 10.8". Figure 2.4 shows the displacements, δ's of all the nonhydrogen atoms of the molecule from the plane through the 11-atom core.

Figure 2.5 shows the conformation of the molecule. All the four octyloxy chains are fully extended and oriented away from the core. The torsional angles presented in Table 2.11 represent the all-*trans* conformation of the chains. The linear end to end dimensions of the molecule calculated as the distances

C(25)...C(70), C(40)...C(55) i.*e.*, length
C(25)...C(40), C(55)...C(70) *i.e.*, width

are 31.6, 31.1, 10.8 and 10.9Å respectively. The average values of the length (31Å) and the width (11Å) of the molecule confers a nearly rectangular shape to the molecule. It must be mentioned that for the mesophase of Cu-OC_8H_{17}, Ohta et *al* [1986] have considered two types of molecular conformations shown in Figure 2.6. Of these, model B strongly resembles the conformation observed by us in

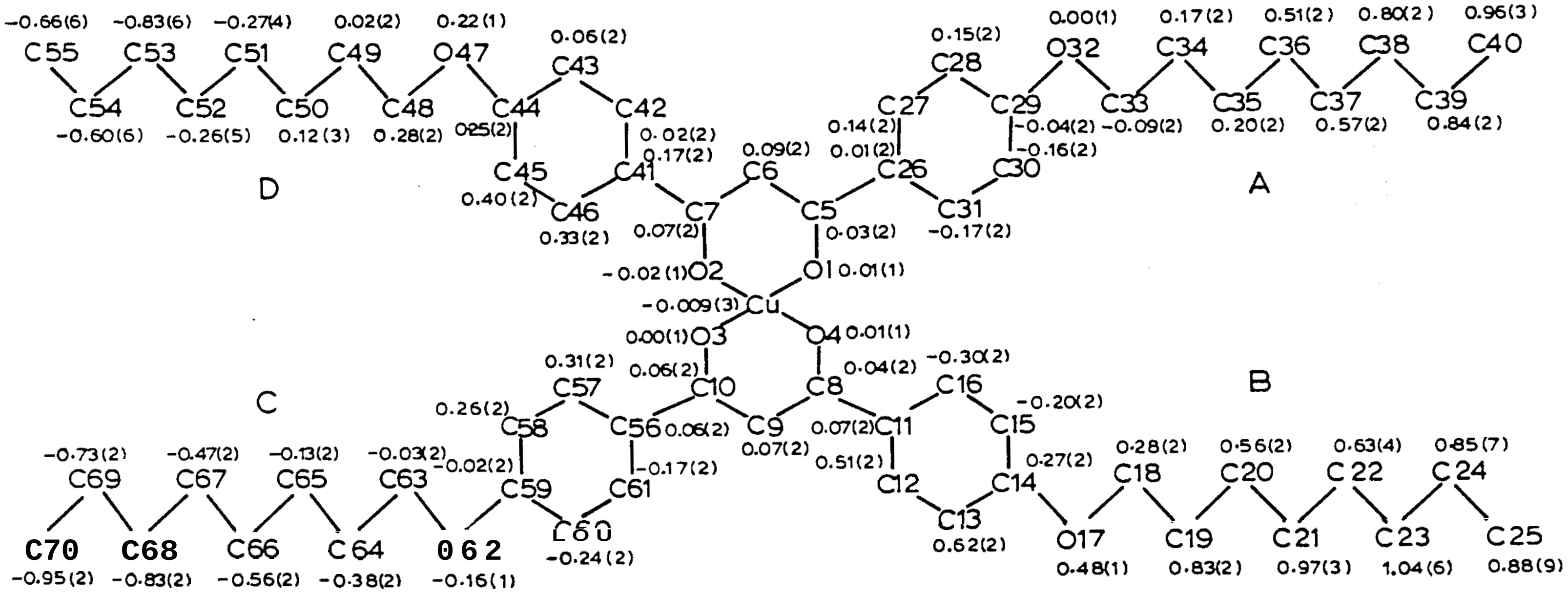

Figure **2.4:** Displacements, 6's of all the nonhydrogen atoms of the molecule from the plane through the 11-atom core.

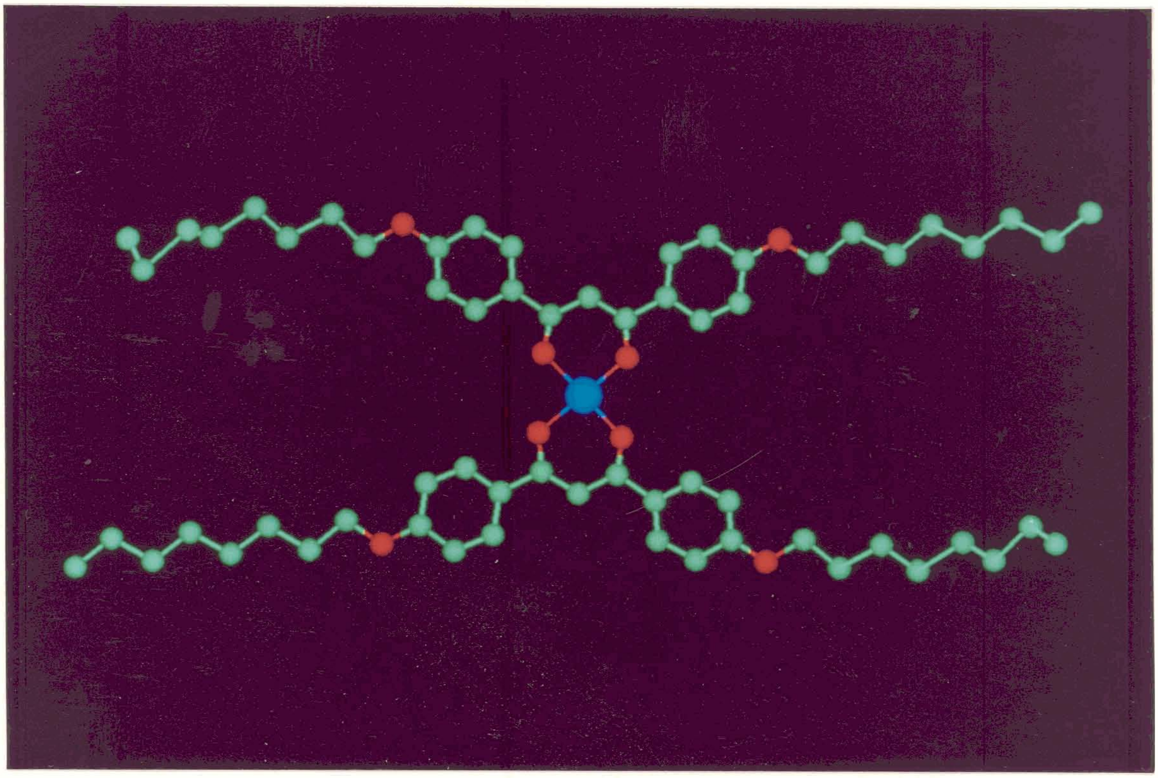

Figure 2.5: Conformation of the molecule.

Table 2.11: Observed torsional angles(°) in the chains.

C(14)-O(17)-C(18)-C(19)	-170(1)	O(47)-C(48)-C(49)-C(50)	178(2)
O(17)-C(18)-C(19)-C(20)	-177(1)	C(48)-C(49)-C(50)-C(51)	174(2)
C(18)-C(19)-C(20)-C(21)	177(2)	C(49)-C(50)-C(51)-C(52)	-175(3)
C(19)-C(20)-C(21)-C(22)	180(2)	C(50)-C(51)-C(52)-C(53)	155(6)
C(20)-C(21)-C(22)-C(23)	-175(4)	C(51)-C(52)-C(53)-C(54)	180(4)
C(21)-C(22)-C(23)-C(24)	172(4)	C(52)-C(53)-C(54)-C(55)	152(5)
C(22)-C(23)-C(24)-C(25)	162(8)	C(59)-O(62)-C(63)-C(64)	-174(1)
C(29)-O(32)-C(33)-C(34)	172(1)	O(62)-C(63)-C(64)-C(65)	-175(1)
O(32)-C(33)-C(34)-C(35)	-176(1)	C(63)-C(64)-C(65)-C(66)	-176(5)
C(33)-C(34)-C(35)-C(36)	178(2)	C(64)-C(65)-C(66)-C(67)	175(2)
C(34)-C(35)-C(36)-C(37)	-179(2)	C(65)-C(66)-C(67)-C(68)	177(2)
C(35)-C(36)-C(37)-C(38)	177(2)	C(66)-C(67)-C(68)-C(69)	180(2)
C(36)-C(37)-C(38)-C(39)	-179(2)	C(67)-C(68)-C(69)-C(70)	174(2)
C(37)-C(38)-C(39)-C(40)	-176(2)		

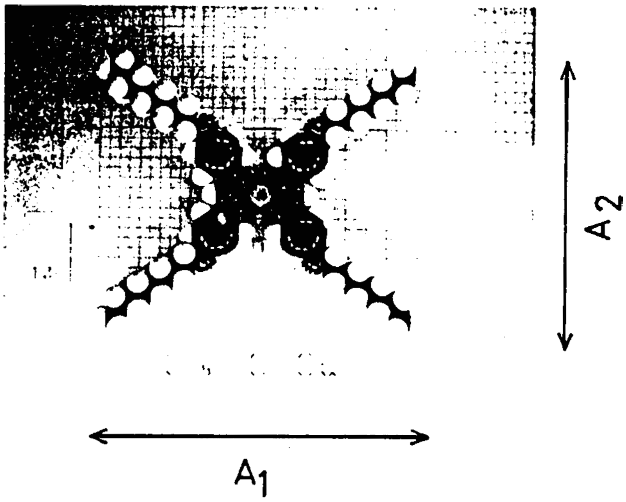

Model A

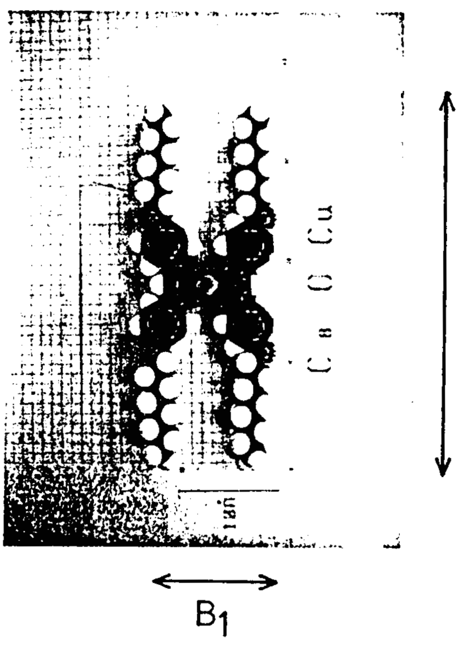

Model B

Figure 2.6: The **models** A and **B for** the molecular conformation **of** Cu-OC_8H_{17} **proposed by** Ohta *et al*, [1986].

the crystalline phase. However, the molecular dimensions via., the length and width of 31 and 11Å respectively, observed in the crystalline phase are significantly less than the corresponding values of 36-36.5 and 15Å, proposed by Ohta et al [1986].

Figure 2.7 shows the molecular arrangement as seen perpendicular to the crystallographic a-axis. The arrangement is essentially layer-like, with the molecules tilted with respect to the crystallographic a-axis (Figure 2.8). As there are two molecules in the unit cell, two layers which are centrosymmetrically related are formed. The molecules in the centrosymmetrically related layers are, however, staggered with respect to each other. This feature is illustrated in Figure 2.7 where the symmetry related molecular pairs are encased within solid lines. The cores of these molecules are parallel, inverted and also slightly staggered with respect to each other. In addition to the layer-like characteristic, the crystal structure of Cu-OC_8H_{17} manifests a columnar character also. The columnar character arises from the periodic repetition of the unit cell contents along the crystallographic a-direction. Thus, the adjacent pairs of layers get regularly stacked along the crystallographic a-direction leading to the formation of infinite columns. This feature is illustrated on the cover of this thesis. It must, however, be pointed out that unlike the case of conventional columnar structures which characterize many discotic mesophases [Chandrasekhar, 1992], in the case of Cu-OC_8H_{17}, the repeat unit of the column is a pair of centrosymmetrically related molecules. The concept of molecular pair is further supported by the concentration of short intermolecular contact distances $\leq$ 4Å, between the two centrosymmetrically related molecules. There are 89 contact distances

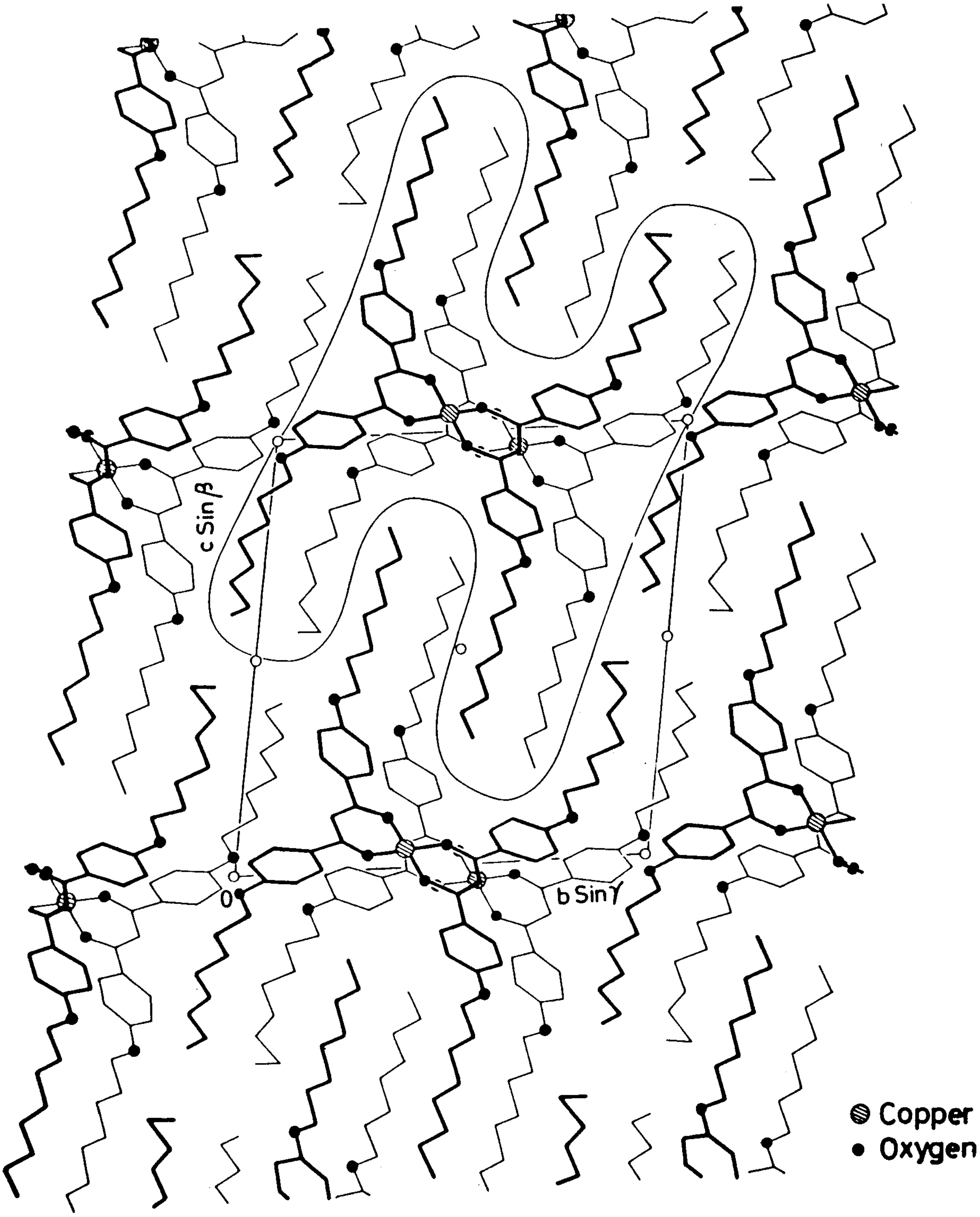

Figure 2.7: Molecular arrangement perpendicular to the crystallographic a-axis

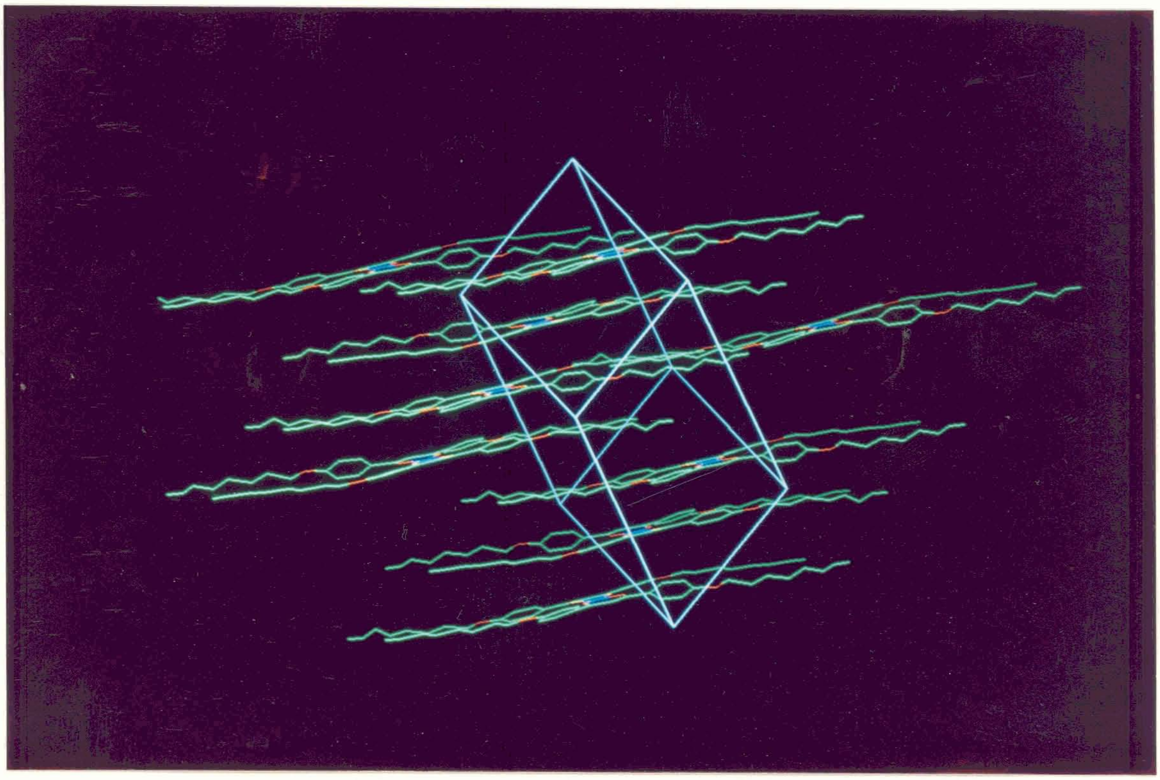

Figure 2.8: View of the layered arrangement of molecules.

between the centrosymmetrically related pairs, of which two are less than the sum of the van der Waal's radii. The number of contact distances between adjacent molecules related by unit cell translation is 15. The preferential occurence of these short contacts between adjacent centrosymmetrically related molecules suggests that they tend to pair. Similar pairing of molecules has been suggested for the discogen, hexa ester of triphenylene [Cotrait et *al*, 1979] which also has a columnar structure in the crystalline phase.

The cores of the above-mentioned molecular pair are tilted with respect to the column axis. Figure 2.9 illustrates the tilted columnar arrangement in a schematic fashion. The angle of tilt, θ, defined as the angle between the column axis and the normal to the plane through the core of the molecule is found to be 128°. Figure 2.7 shows that the interior of each column is made up of the nearly-rigid core of the molecule and also the phenyl rings. The octyloxy chains constitute the periphery of each column. Figure 2.7 also shows that each column in the crystal structure is surrounded by six others situated at $\pm\vec{b}$, $\pm\vec{c}$ and $\pm(b+c)$. Obviously the arrangement of the six coordinating columns does not correspond to a regular hexagon. In the crystal lattice, the rigid, central regions of adjacent columns are separated by distinct pockets made up of aliphatic chains (Figure 2.7). Thus, the column...column interactions appear to be essentially of the chain...chain type of non-bonded van der Waal's interactions.

Figure 2.9 shows the zig-zag arrangement of copper atoms about the column axis. The sig-zag distances are 6.3 and 6.6Å respectively and the angle at the zig-zag is 124°

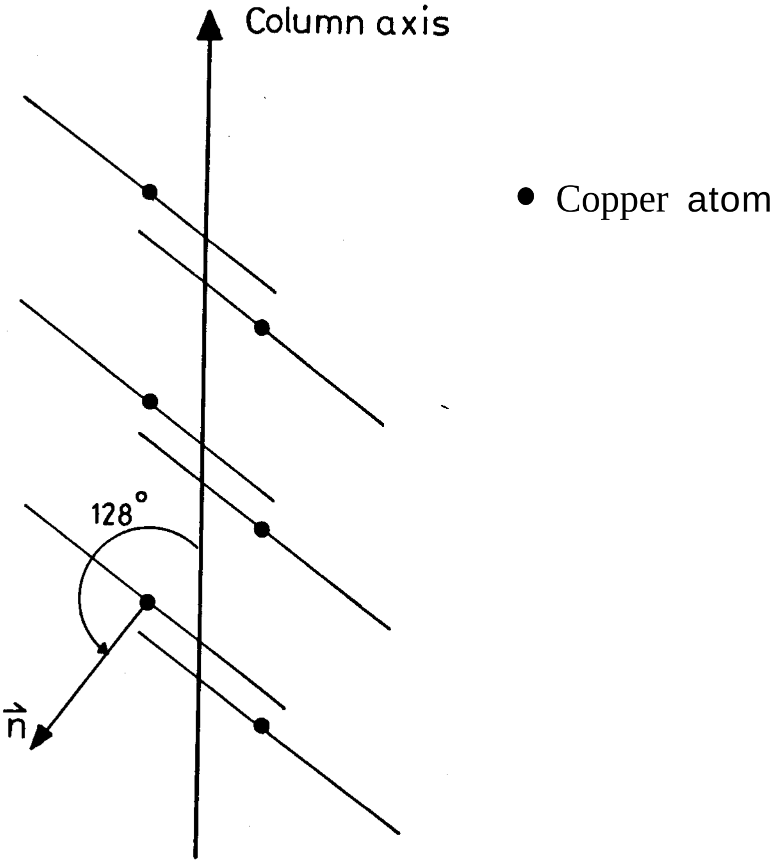

Figure 2.9: Schematic diagram of the columnar arrangement of the molecular pair. The copper atoms are distributed along the column axis in a zig-zag fashion.

In section 2.2 of this chapter, it was pointed out that the comparatively high value of $\sigma(a)$ (Table 2.1) may be correlated with the molecular arrangement in the crystal lattice. Details of the columnar arrangement described in the previous paragraphs suggest that the column axis is perhaps the direction along which preferential slip or sliding between adjacent columns can occur. As the crystallographic a-axis coincides with the column axis, presence of such a "disorder" can be expected to manifest as lowering of the accuracy of the unit cell translation along this direction. It is also noticed from Table 2.7 that the e.s.d's of the x coordinates are generally higher than those of y and z coordinates of the atoms. It is admitted that the above mentioned explanation is not conclusive and it merits further detailed study of the possible slip between adjacent columns.

2.4.1 Structural characteristics of the crystalline and the mesophases

X-ray study of the mesophase of Cu-OC_8H_{17} has been carried out by Ohta et *al*, [1986]. They have observed four reflections the d-spacing of which are in the ratio of $1 : \frac{1}{2} : \frac{1}{3} : \frac{1}{4}$, based on which they propose a lamellar structure for the mesophase. Using space filling models, they have also calculated the length and the width of the molecule. They have considered two possible conformations referred to as models A and B respectively (Figure 2.6). Table 2.12 compares the dimensions of these models with that observed by us in the crystalline phase. To accomodate a molecule whose length, L is larger than the mesophase layer thickness, W of 23Å. Ohta et *al*, [1986], propose a tilted arrangement of molecules,

Table 2.12: Comparison of the molecular dimensions of $Cu\text{-}OC_8H_{17}$.

	length (A)	**breadth** (A)
(Ohta *et al*, 1986)'s		
Model **A**	**32.0**	27.5
B	**36.0-36.5**	**15.0**
Crystal	31	11

illustrated in Figure 2.10(a). With the tilted layer structure, the angle of tilt ψ is 46° for model A and $\sim$ 40° for model B.

Comparison of the above mentioned details about the mesophase with those of the crystalline phase has led to the identification of some interesting features which favour the possibility of direct correlations existing between the structural characteristics of the crystalline and the mesophases of Cu-OC_8H_{17}.

(i) layer structure:

As mentioned earlier, the crystal structure of Cu-OC_8H_{17} has both layer-like and columnar characteristics. During the thermally induced crystalline to mesophase transition, if the thermal energy is sufficient to disturb the periodic stacking of the layers, the columnar arrangement could be lost, and only the layer structure may be retained in the mesophase. The high value of σ(a) mentioned earlier supports the possibility of the periodic stacking along the a-axis getting disturbed. Thus, the transformation from the columnar structure in the crystalline phase to the layer structure in the mesophase is likely to be through the weakening or removal of the forces which are responsible for the stacking of molecules.

(ii) Conformation of the molecule:

The dimensions listed in Table 2.12 show that for model A, the length to width ratio is $\sim$ 1.2 whereas for model B, the ratio is $\sim$ 2.4. The length to width ratio of the molecule as observed from the crystal structure is $\sim$ **3** and compares reasonably well with corresponding value for model B. It is therefore likely that in the mesophase also the molecular conformation resembles model B.

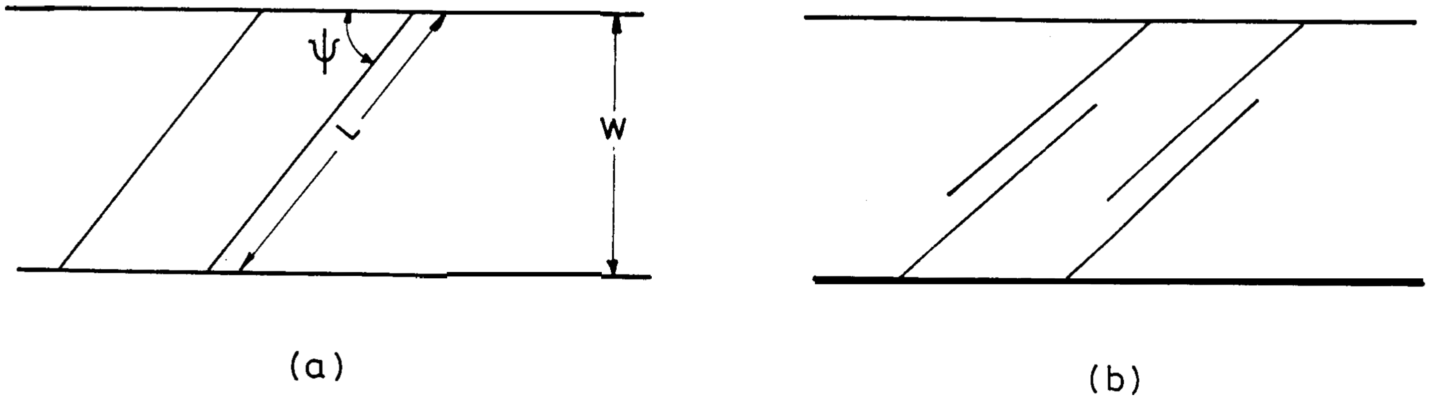

Figure 2.10: Schematic representation of the tilted arrangement of molecules in a layer constituted by (a) single molecules [Ohta et *al*, 1986]) (b) molecular pairs.

(iii) Tilt in the layer structure:

The columnar structure observed in the crystalline phase of Cu-OC_8H_{17} (Figure 2.9) shows that the layer thickness is ~ 25Å. This value compares well with the thickness of 23Å obtained by Olita *et al* [1986], using the X-ray data from the mesophase. If the 31Å long molecules are to be arranged in a layer of thickness 238, the till within the layer turns out to be ~ 48° calculated using the relation, $\psi = sin^{-1}\left(\frac{23}{31}\right)$. This value is more than the till of ~ 40° proposed by Ohta et al, [1986]. If, however, the pairing of molecules observed in the crystalline phase is retained in the mesophase also, the effective length of the staggered molecules increases (Figure 2.10(b)) and consequently the tilt angle ψ within the layer would also decrease.